Biophysical Chemistry 290 (2022) 106879

Contents lists available at ScienceDirect

Biophysical Chemistry

journal homepage: www.elsevier.com/locate/biophyschem

Fluorescence interactions of a novel chalcone derivative with membrane model systems and human serum albumin

Berat Yildirim [a], Burcu Meryem Beşer [a,*], Nevin Ulaş Çolak [b], Ahmet Altay [a], Ahmet Yaşar [b]

[a] Faculty of Arts and Sciences, Department of Chemistry, Erzincan BinaliYıldırım University, Erzincan, Turkey
[b] Faculty of Pharmacy, Department of Analytical Chemistry, Karadeniz Technical University, Trabzon, Turkey

ARTICLE INFO

Keywords:
Cell staining
Chalcone
Fluorescence energy transfer
Human Serum Albumin (HSA)
Micelle

ABSTRACT

A novel chalcone derivative (4-(5-(pyridin-2-yl)-4,5-dihydro-1H-pyrazol-3-yl) phenol (PDP) was synthesized, characterized and investigated for its potential as a fluorescent probe. The structure of the synthesized molecule was determined by FTIR, ^{1}H NMR, ^{13}C NMR and LC-MS/MS. The interactions of PDP with fluorescent dyes in aqueous SDS environment and HSA were studied by using fluorescence resonance energy transfer (FRET) technique and steady-state and time-resolved fluorescence spectroscopy techniques. In addition, the cytotoxic effects of PDP against various cell lines (MCF -7, HT −29, and 3 T3-L1) as well as their corresponding healthy cell lines were tested by MTT assay and visualization of FRET efficiency of PDP in vitro was monitored by confocal microscopy. MTT assay showed that PDP has no significant cytotoxic effect on HT −29 cancer cells and moderate cytotoxicity on MCF -7 and 3 T3-L1 cells even at a concentration of 250 μM. Combining confocal microscopes with the FRET technique showed that PDP significantly stained the cytoplasm of MCF -7 cell lines. These results suggest that PDP could be used in fluorescence microscopy for cell staining.

1. Introduction

In the modern era, dyes have extensive application in a variety of commercial industries such as cosmetics, textile, food, printing, and electronics. Apart from industrial usage, dyes with specific photophysical and electrochemical properties are important for applications in both biochemistry and physical chemistry. Organic dyes are called choromophores which literally means “carriers of color”. They have conjugated π-systems and absorption of certain wavelengths of visible light leads them to change color [1]. One class of choromophores that exhibit chromophoric properties are chalcones which are aromatic compounds ubiquitous in plants. They are the precursors of flavonoids and chemically two aromatic rings are joined to form a three-carbon α, β-unsaturated carbonyl system [2]. Chalcones are bioactive scaffolds of medical interest due to their great deal of pharmacological and biological activities. They have a 1,3-diaryl-2-propen-1-one carbon structure and the presence of the unsaturated ketone moiety confers biological activity to the chalcones [3]. They are well known to have antimicrobial, antiviral, antifungal, anticancer, antitubercular, antioxidant, anti-inflammatory, antileishmanial and other important biological activities [4–7].

Chalcones could be easily obtained by Claisen-Schmidt condensation between ketones and aromatic aldehydes [8]. The increasing interest to synthesize pyrazoline derivatives is due to the two main reasons [9]. The first is that they have some pharmacological activity, and the second is that they can be used as fluorescent probes because they have electron donors and acceptors. This makes them ideal candidates for fluorescence resonance energy transfer (FRET) applications.

FRET is a photophysical phenomenon in which energy is transferred from an excited donor fluorophore to a ground state acceptor fluorophore via non-radiative processes, allowing the quantification of the transferred energy with and an eq. [10]. FRET is accurate, reliable and efficient when the fluorescence emission spectrum of donor molecule overlaps at least 30% with the fluorescence excitation spectrum of the acceptor molecule [11]. With this technique, it is possible to accurately obtain spatial measurements of molecules at over distances from 10 to 100 A°. Although FRET was initially considered as a physical event, it was later put into practice as extremely useful tool to understand bimolecular interactions. Over the past decades, FRET technique has been widely used in various heterogeneous aggregated environments such as micelles, vesicles, proteins, lipids, DNA, nucleic acid, microemulsions [12]. Since the molecular environment around the

* Corresponding author.
E-mail addresses: berat.yildirim@worldmedicine.com.tr (B. Yildirim), baydin@erzincan.edu.tr (B.M. Beşer), nevinulas@ktu.edu.tr (N.U. Çolak), aaltay@erzincan.edu.tr (A. Altay), ahmetyasar@ktu.edu.tr (A. Yaşar).

https://doi.org/10.1016/j.bpc.2022.106879
Received 3 June 2022; Received in revised form 23 August 2022; Accepted 24 August 2022
Available online 27 August 2022
0301-4622/© 2022 Elsevier B.V. All rights reserved.

fluorescence probe could affect the interaction between donor and acceptor as well as the florescence parameters, two major systems have been utilized to study the fluorescence character of a potential probe: surfactant micelle systems and protein binding systems.

Surfactants consist both polar and apolar fragments. Having hydrophobic tails and hydrophilic heads, surfactants at appropriate concentrations form regular structures [13–16]. Monolayer structures are called micelles, reverse micelles and bilayer structures are called liposomes. As liposomes resemble the artificial phospholipid bilayers, they exhibit biocompatible properties and become a simple model for cell membrane [17]. In addition, in vitro systems are excellent models that are currently used to investigate the photophysical characteristics of dye molecules and are extremely useful for mimicking the in vivo systems [18–21]. Interactions of organic dyes with bio-macromolecules have significantly contributed our understating on the mechanism of biophysical process in living systems. Human serum albumin (HSA) is a major soluble protein found in blood plasma [22–24]. Having various physiological functions, HSA plays important role in osmotic pressure and transportation of various ligands such as fatty acids, amino acids steroids and metals like copper, zinc to specific targets [25]. This could be due to the fact that there is a hydrophobic pocket inside the protein network of HSA and it has the flexibility of adapting its shape when interacting various small molecule, drug and other bioactive molecules [26].

Since fluorescence-based techniques are widely used to measure sensitively the dynamics of biological processes and functions at the molecular level, FRET has been also applied to in vitro systems. FRET combined with fluorescence microscopy techniques allowed real-time measurement of living cells, opening a new avenue in investigating the choice of new fluorophores [27,28].

Although the dyes with specific photophysical and electrochemical properties are important for applications in both biochemistry and physical chemistry, it is very difficult to obtain organic dyes that are not harmful to nature. In addition, the isolation and purification of organic dyes require high cost. On the other hand, the synthesized dyes may cause pollution problems, depletion of natural resource affecting ecological balance. Therefore, it is important to examine the cytotoxic effects of new organic dyes [29–31]. The production of a fluorescent probe, which can be synthesized with an easy and inexpensive technique, is non-cytotoxic, with well-defined photophysical properties will provide an advantage over the molecules in the literature.

Overall, our goal in this work was to explore the potential of PDP as a biological fluorescent probe by investigating different aspects of PDP. For this reason, we performed this study in four steps: (i) we synthesized and characterized PDP; (ii) we tested the FRET capacity of PDP in a surface-active micelle system; (iii) we investigated a possible FRET interaction between PDP and HSA; (iv) we investigated the safety of PDP by studying its cytotoxic effects on three cancer cell lines compared to the corresponding healthy cell lines; and finally (v) to see if PDP can be used to stain cells, we monitored confocal images of breast cancer cells based on the FRET technique.

2. Material and method

2.1. General procedure for the synthesis of chalcone derivative (4-(5-(pyridin-2-yl)-4,5-dihydro-1H-pyrazol-3-yl) phenol (PDP)

PDP has been selected to investigate its fluorescent probe potential (Empirical Formula: $C_{32}H_{24}N_5Br$). The molecular structure of PDP is given in Fig. 1. The target molecule was successfully synthesized based on synthetic route as illustrated in Scheme 1. Chalcone derivative was synthesized by the reaction of 2-hydroxyacetophenone with 4-pyridinecarboxaldehyde with %56 yield. Then using hydrazine hydrate, the reaction mixture was stirred at 70 °C for 4 min at the microwave (800 watt) and the final product was obtained. Characterization of PDP was established with the spectra of FT-IR, ^{1}H NMR, and ^{13}C NMR.

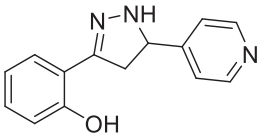


Fig. 1. Structure of 4-(5-(pyridin-2-yl)-4,5-dihydro-1H-pyrazol-3-yl.

NMR spectra were recorded using a Varian Mercury NMR at 200 MHz in $CDCl_3$. NMR peaks were assignment using ^{1}H, 1^3C, APT, ^{1}H—^{1}H COSY, and ACD NMR program. The elemental analyses were achieved on a Costech ECS 4010 instrument. Infrared spectra were obtained with a Perkin-Elmer 1600 FT-IR (4000–400 cm^{-1}) spectrometer. Melting points were determined by using a Thermo-var apparatus fitted with a microscope and are uncorrected. UV-VIS spectral analyses were carried out on a Unicam UV2–100 at 25 °C. The reactions are carried out in DBK manual microwave instrument (800 W). Thin-layer chromatography (TLC) was carried out on Merck precoated 60 Kieselgel F254 analytical aluminum acidic or basic plates.

Brown, melting point 167.7 °C; UV λ^{CHCl3}max nm: 386 (ε, 3860), 294. **FT-IR** (KBr): NH:2984,C=N:1596,OH:3195. **^{1}H NMR** (200 MHz, CDCl3, ppm): 4.84 (t, $J = 8.0$ Hz 1H, H-3), 6.69 (d, $J = 8.0$ Hz, 1H, H-3), 2.83 (dd, $J = 12.0$ Hz, $J = 28$ Hz, 1H, H-4a), 3.48 (dd, $J = 12.0$ Hz, $J = 28$ Hz, 1H, H-4b), 7.44(s, 1H, H-2′), 7.12 (d, $J = 8$ Hz, $J = 2.0$ Hz, 1H, H-4′), 7.25 (t, $J = 16.0$ Hz, $J = 8.0$ Hz 1H, H-5′), 7.82 (d, $J = 8$ Hz, Hz, 1H, H-6′), 8.52 (d, $J = 4$ Hz, 1H, H-2″), 7.37 (d, $J = 4$ Hz, 1H, H-3″), 7.37 (d, $J = 4$ Hz, 1H, H-5″), 8.52 (d, $J = 4.0$ Hz, 6″), 2.30(s 3H -CH3), 5.10 (s, 1H, -NH). **^{13}C NMR** (50 MHz, CDCl3, ppm): 180.81C=O, 129.20 C2(Cα), 134.75 C3(Cβ), 138.06 C1', 128,86 C2', 133.35 C3', 129.32 C4', 126.52C5', 126.24 C6', 149.25 C1" (C1), 119.87 C2" (C2), 150.17 C3" (C3), 150.17 C5" (C5), 119.87 C6".

2.2. Chemicals

Fluorescein (Fl), Pyronin Y (PyY), Acridine Orange (AcO), Safranin T (SfT), Sodium Dodecyl Sulfate (SDS) (surfactant), Human Serum Albumin (HSA) and reference compound Quinine Sulfate were obtained from Sigma-Aldrich and all chemicals are spectroscopic grade.

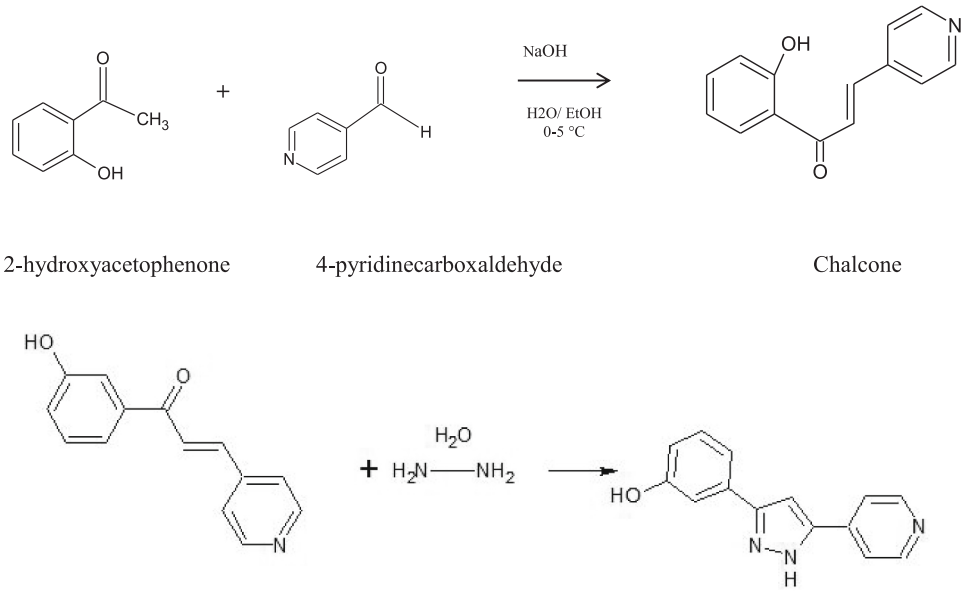
Dye solutions (1.0×10^{-3} M) and PDP solution (1.0×10^{-4} M) were prepared as stock solutions in 2:1 ethanol–chloroform mixture and kept in dark. A preliminary study was carried out determine the concentration range of SDS. The critical micelle concentration of SDS was determined as 8.1 mM and the working concentration of SDS was determined as 8.5 mM. Phosphate buffer was prepared by dissolving one PBS tablet in 200 mL of deionized water using an ultrasonic bath. HSA solutions were freshly prepared in phosphate buffer (1.0×10^{-6} M, pH = 7.4). Solutions were prepared in deionized water, just prior to spectroscopic measurements.

3. Experimental

For the experimental part, 1.0×10^{-4} M PDP was pipetted and dried with argon gas, then increasing concentrations of dye solutions were added with automatic pipettes. Lastly the prepared SDS solution was added and the total volume was adjusted to 4.0 mL. The prepared samples were kept in an ultrasonic bath for 15 min before each measurement in order to completely dissolve the dye (SfT, AcO, PyY, Fl) and PDP in the solution. To measure the effect of temperature on the UV and fluorescence measurements, temperatures (25, 35 and 45 °C) were kept constant using a temperature-controlled magnetic stirrer.

3.1. Instrumentation

The UV- absorption spectra of Fluorescein (Fl), Pyronin Y (PyY), Acridine Orange (AcO), Safranin T (SfT) at different concentrations were



Scheme 1. Synthesis of 4-(5-(pyridin-2-yl)-4,5-dihydro-1H-pyrazol-3-yl.

monitored using T80+ uv/vis spectrophotometer (PG Instrument). Fluorescence experiments were performed at 25° ± 0.1 °C using a Shimadzu spectrofluorometer (Shimadzu RF-5301 PC Spectrofluorophotometer (Japan)). Fluorescence lifetimes were monitored according to the single photon counting technique using Horiba-Jobin-Yvon-SPEX Fluorolog 3-2iHR instrument equipped with time-correlated single photon counting controller (TCSPC) at excitation wavelength of 310 nm and emission wavelength of 460–475 nm. Fluorescence measurements of each sample were taken and recorded for three times.

3.2. In vitro cytotoxicity assay

In vitro cytotoxic effects of PDP on colorectal adenocarcinoma cell lines(HT-29) and breast cancer cell lines (MC-7) 3 T3-L1 were measured by the XTT method according to the manufacturer's instructions (Cell Proliferation XTT Kit, BI). Carcinoma cells were seeded in 96-well (Sarstedt, Numbrecht, Germany) at a density of 10,000 cells/well in a total volume of 100 µL. After 2 h of incubation (at 37 °C in a 95% humidity and in an atmosphere containing 5% CO_2), the medium was removed from the adherent cells and the wells were washed with 50 µL PBS buffer. Then, 50 µL of fresh medium was added per well followed by 50 µL of sample (PDP) at two concentrations (100–250 µM). After 24 h of incubation, the medium in each well was removed. Then, 100 µL of basal medium and 50 µL XTT solution were added to each well. To the control wells, 100 µL of complete medium containing 0.2% DMSO was added. The plate was placed in a CO_2 incubator for 5–6 h. Finally, the absorbances at 450 nm (reference filter at 650 nm) were measured at in an ELISA reader (Anthos-HTII) and cell viability in the wells was calculated.

3.3. Confocal microscopy imaging

MCF -7 Cells were cultured in DMEM containing high glucose supplemented with 10% FBS, 1% penicillin/streptomycin, and 200 mM L-glutamine at 37 °C with 95% humidity and 5% CO_2. When the cells reached 85–90% confluence, the attached cells were trypsinized and removed from the culture flasks. They were seeded onto the glass slides at an initial cell density of 1×10^5 cells/well. After 24 h of incubation, the cells were fixed with 4% paraformaldehyde for 30 min. Then, 100 µL of 100 µM PDP was added to the cells and incubated in the dark for 15 min. These images of the cells were taken at 360 nm excitation and 650 nm emission using a confocal laser scanning microscope (Zeiss LSM 710) at 20× magnification.

3.4. Statistical analysis

Statistical analyses of the cytotoxicity assays were performed by one-way ANOVA with unpaired *t*-test using statistical program GraphPad Prism 6 (GraphPad, La Jolla, CA) Software 7.0). All results were expressed as means with their standard deviation (±SD). $p < 0.05$ was considered as the minimum level of significance.

4. Results

4.1. PDP-dye interactions in micelle system

4.1.1. Absorption and fluorescence spectral properties

In the first stage of our study, fluorescence energy transfer was investigated in SDS environment, which is one of the micellar systems accepted as biological membrane model. In order to observe the spectral overlap correctly, the spectra are normalized and shown on the same graph (Fig. 2). It can be seen that the fluorescence spectrums of PDP overlaps absorption spectra of AcO, Fl, PyY, SfT dye molecules, which indicates that PDP is relevant for energy transfer studies.

Next, the fluorescence spectrums of the donor PDP and the acceptor (AcO / Fl /PyY /SfT) absorption spectra were examined. For this reason, the concentration of PDP, acting as donor, was kept constant (1.0×10^{-4}M) and increasing concentrations of dye molecules (SfT, AcO, PyY and Fl), acting as acceptor molecules, were added to 8.5 mM SDS medium and fluorescence measurements were taken (λex = 350 nm; λem = 365-690 nm).

The emission spectra are shown in raw form, without normalization in Fig. 3. The isosbestic point is the wavelength at which the light absorption remains constant even if the concentration of a solution changes. Isosbestic points were observed at 504 nm, 538 nm and 541 nm for AcO, PyY and SfT, respectively. However, the isosbestic point could not be observed in PDP and Fl molecule pair (Fig. 2B). By examining the spectra (Fig. 2), it was observed that the fluorescence intensity of PDP at constant SDS concentration decreases with the increase in the concentration of AcO and SfT. In these two spectrums, it was observed that a new band was formed with a peak maximum around 520–525 nm and

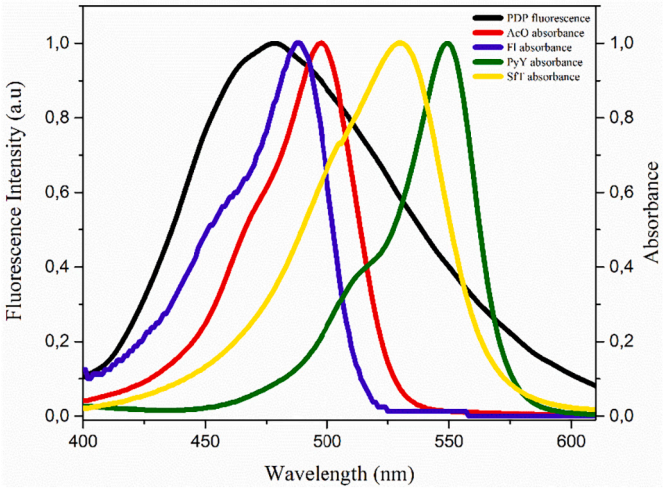


Fig. 2. The normalized spectral overlap of PDP emission and SfT, AcO, PyY, Fl absorption in SDS ($C_{PDP} = 1.0 \times 10^{-4}$ M $C_{AcO/Fl/PyY/SfT} = 1.0 \times 10^{-5}$ M, SDS = 8.5 mM).

566–571 nm, which shows fluorescence peak of the AcO and SfT, respectively. When the spectrum of PDP and PyY molecules and PDP and Fl are examined, although there is no significant decrease in the peak intensity of PDP at a constant concentration, the peak of the acceptor molecules (PyY, Fl) are quite strong: 566–569 nm and 504–512 nm, respectively.

4.1.2. *Fluorescence quantum yields*

Fluorescence quantum yields are measured to see the efficiency of the fluorescence process [32]. It is defined by the ratio of the number of emitted photons to the number of absorbed photons per time unit.

$$\Phi_F = \text{Number of emitted photons}/\text{Number of absorbed photons} \quad (1)$$

Quantum yields are critical because they are used to characterize a substance under certain conditions and to calculate quenching-rate constants, energy transfer, lasing ability, and radiative and non-radiative rate constants, each of which indicates different aspects of photophysical properties of a substance [33]. Fluorescence quantum yield of a fluorescent compound varies depending on the solvent used, the temperature of the environment, the rigidity of the molecule, the heavy metals in the molecular structure, and the atom or atom groups

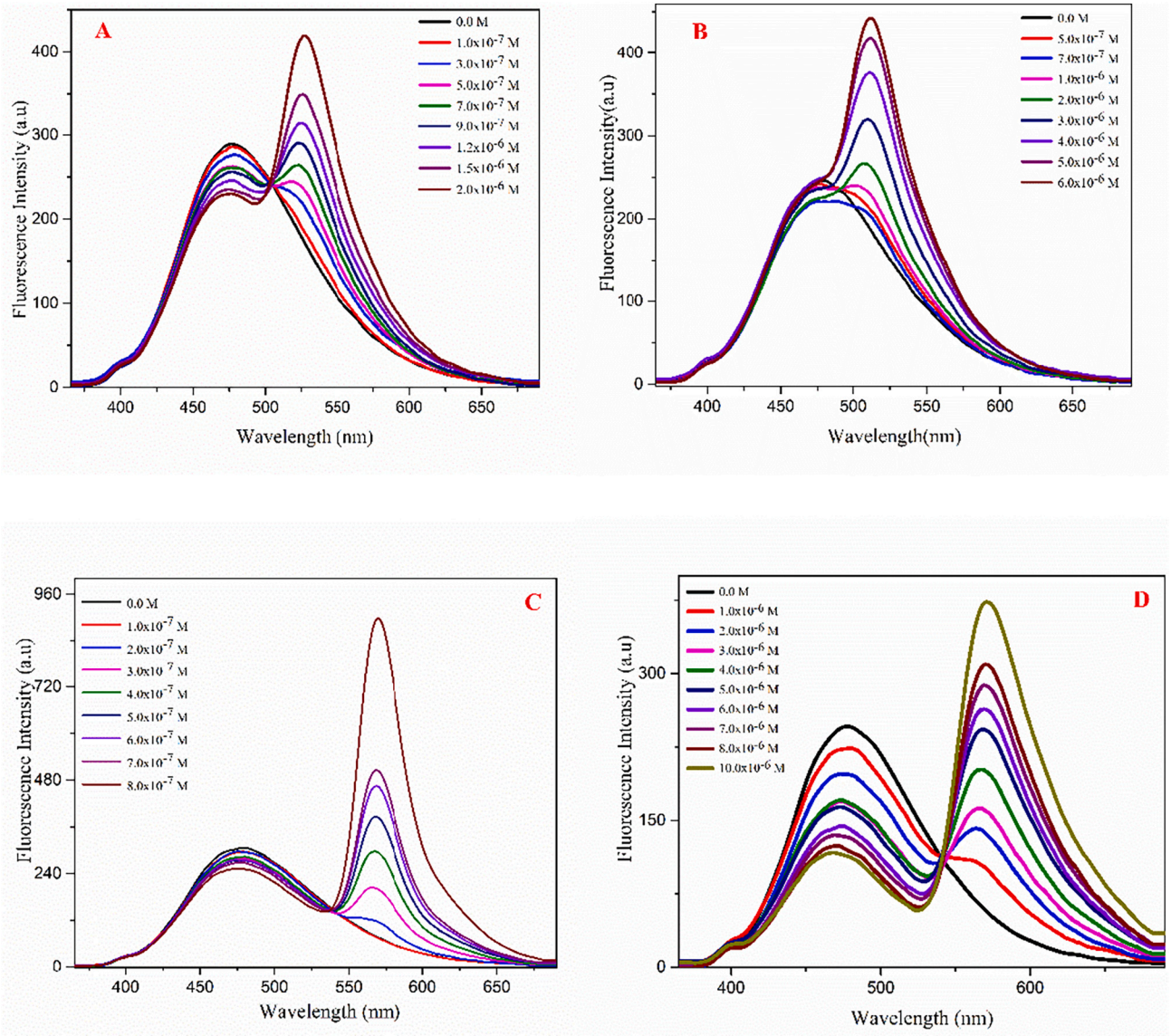


Fig. 3. FRET profile of PDP with increasing dye concentration at room temperature (≈25 °C) AcO (A), Fl (B), PyY (C) and SfT (D), λ_{ex} = 370 nm.

that have electron pairs in the structure of the molecule. One of the most frequently used methods when determining the fluorescence quantum yields of systems without reaction is the Parker-Rees method [34], which has been used in this study. This method requires a reference fluorescent compound with a well-defined photophysical property. Here we used quinine sulfate solution as reference to estimate the fluorescence quantum yield. Other suitable reference or standard compounds are given in the literature [35]. First, the absorption of reference solutions and the sample solution are recorded, then the emissions of these solution are recorded and finally the areas under the curves are measured. Parker-Rees equation is expressed as following:

$$\phi_s = \phi_r \left(\frac{D_s}{D_r}\right)\left(\frac{n_s}{n_r}\right)^2 \left(\frac{1-10^{-OD_r}}{1-10^{-OD_s}}\right) \quad (2)$$

where, ϕ_s and ϕ_r are the fluorescence quantum yield of the sample and the reference, D_s and D_r are the areas under the corrected fluorescence spectrum of the sample and the reference, n_s and n_r are the refractive index of the sample and the reference solvent, OD_s and OD_r are the optical density measured at the excitation wavelength of the sample and the reference, respectively.

Fluorescence quantum yields of the PDP with Fl, PyY, AcO and SfT dyes at different concentrations in the micellar system (SDS) are given in Table 1. It can be seen that, in SDS environment, the quantum yields of the PDP decrease with the addition of increasing concentrations of dyes (AcO, Fl, PyY and SfT) to the medium, which means that the dyes act as quenchers and quenching occurs.

4.1.3. Energy transfer parameters (J and R)

The extent of energy transfer depends on the distance between donor and acceptor (typically in the range of 1–10 Å) and the spectral overlap of donor' emission spectrum and acceptor' absorption spectrum [27]. We have determined the energy transfer parameters for PDP in the presence of different dyes by calculating R, J and E. R_o is called the Förster radius, which is the distance between the donor and acceptor molecules at which the efficiency of energy-transfer is about 50%. It can be calculated using the following equation:

$$R_0^6 = 8.8x10^{-25}k^2N^{-4}\phi J \quad (3)$$

where κ^2 is spatial orientation factor of the dipole, N is refractive index of the medium, Φ is the fluorescence quantum yield of the donor, and J is the overlap integral of the fluorescenceemission spectrum of donor and absorption [36]. The J value represents the size of the spectral overlap area, which indicates the probability of energy transfer to occur J is given by the following equation:

$$J = \frac{\sum F(\lambda)\varepsilon(\lambda)\sigma\lambda^4\Delta\lambda}{\sum F(\lambda)\Delta\lambda} \quad (4)$$

where $F(\lambda)$ is the fluorescence intensity of the fluorescent donor of wavelength λ, $\varepsilon(\lambda)$ is themolar absorption coefficient of the acceptor at wavelength λ. The energy transfer efficiency is determined by the following equation:

$$E = 1 - \frac{F}{F_0} = \frac{R_0^6}{R_0^6 + r^6} \quad (5)$$

This equation tells us that if the distance between donor and acceptor is about R_0 than even a minor change in the distance significantly affect the energy transfer efficiency since FRET efficiency is inversely proportional to the sixth power of the distance [37].

The calculated Ro is usually lie between 15 and 60 Å range and it is useful for elucidating the proximity of two molecules in response to macromolecular association and major conformational changes. If the separation distance between donor and acceptor is >80 Å the sensitivity of FRET lowers. In this study as can be seen from the Table 2 the estimated distances between donor and acceptor are well in the range which indicates that FRET is well operational in these systems.

4.1.4. Fluorescence quenching mechanism (Ksv, kq, Ka, E, r(Å), n, R^2)

Fluorescence quenching is a process that the fluorescence intensity of the sample solution decreases which may occur as a result of different form of molecular interactions. There are two type of quenching mechanisms: dynamic quenching and static quenching. In dynamic quenching interaction between fluorophore and the quencher occurs during the lifetime of the excited state whereas static quenching happens at ground state [38]. In other words, static quenching refers to formation of a complex between the fluorophore and quencher, whereas dynamic quenching is a collisional process. The quenching data can be deducted from the Stern–Volmer equation.

$$\frac{I_0}{I} = \frac{F_0}{F} = 1 + k_q\tau[Q] = 1 + K_{SV}[Q]\ k_q = \frac{K_{SV}}{\tau_0} \quad (6)$$

where; F_0 (I_0) and F (I) are fluorescence intensities in the absence and presence of quencher in the environment; kq, bimolecular quenching constant; K_{SV} is the Stern-Volmer constant, τ, the time the fluorophore spent in the excited state in the absence of the quencher or the fluorescence lifetime of the fluorophore, Q, quencher's concentration; and $K_{SV} = kq.\tau$ represents the Stern-Volmer constant.

Stern–Volmer quenching values of PDP-dye pairs were obtained from the slope of the graphs at all temperatures (from Eq. (6) and Fig. 4) and listed in Table 3.

The linear observation of the Stern-Volmer plot cannot discriminate

Table 2
Energy transfer parameters for PDP-Dye(s) system.

	J ($M^{-1}cm^{-1}nm^4$)	R_0 (Å)
PDP + AcO	2.12×10^{-15}	49.98
PDP + SfT	2.48×10^{-15}	51.3
PDP + PyY	1.48×10^{-15}	47.06
PDP + Fl	2.08×10^{-15}	49.8

Table 1
Fluorescence quantum yields of PDP at different concentrations in micellar system with Fl, PyY, AcO and SfT.

PDP							
[SfT] / M	ϕ_f	[AcO] / M	ϕ_f	[PyY] / M	ϕ_f	[Fl] / M	ϕ_f
0	0.254 ± 0.005	0	0.254 ± 0.005	0	0.254 ± 0.005	0	0.254 ± 0.005
1.0×10^{-6}	0.220 ± 0.008	1.0×10^{-7}	0.250 ± 0.003	1.0×10^{-7}	0.244 ± 0.002	5.0×10^{-7}	0.218 ± 0.006
2.0×10^{-6}	0.190 ± 0.007	3.0×10^{-7}	0.231 ± 0.006	2.0×10^{-7}	0.207 ± 0.002	7.0×10^{-7}	0.196 ± 0.005
3.0×10^{-6}	0.154 ± 0.005	5.0×10^{-7}	0.227 ± 0.002	3.0×10^{-7}	0.203 ± 0.003	1.0×10^{-6}	0.189 ± 0.002
4.0×10^{-6}	0.146 ± 0.002	7.0×10^{-7}	0.223 ± 0.003	4.0×10^{-7}	0.198 ± 0.002	2.0×10^{-6}	0.145 ± 0.005
5.0×10^{-6}	0.142 ± 0.001	9.0×10^{-7}	0.215 ± 0.004	5.0×10^{-7}	0.193 ± 0.003	3.0×10^{-6}	0.138 ± 0.002
6.0×10^{-6}	0.125 ± 0.005	1.2×10^{-6}	0.199 ± 0.001	6.0×10^{-7}	0.187 ± 0.001	4.0×10^{-6}	0.123 ± 0.005
7.0×10^{-6}	0.115 ± 0.004	1.5×10^{-6}	0.184 ± 0.005	7.0×10^{-7}	0.187 ± 0.002	5.0×10^{-6}	0.109 ± 0.002
8.0×10^{-6}	0.106 ± 0.004	2.0×10^{-6}	0.176 ± 0.004	8.0×10^{-7}	0.173 ± 0.005	6.0×10^{-6}	0.094 ± 0.003
1.0×10^{-5}	0.099 ± 0.001						

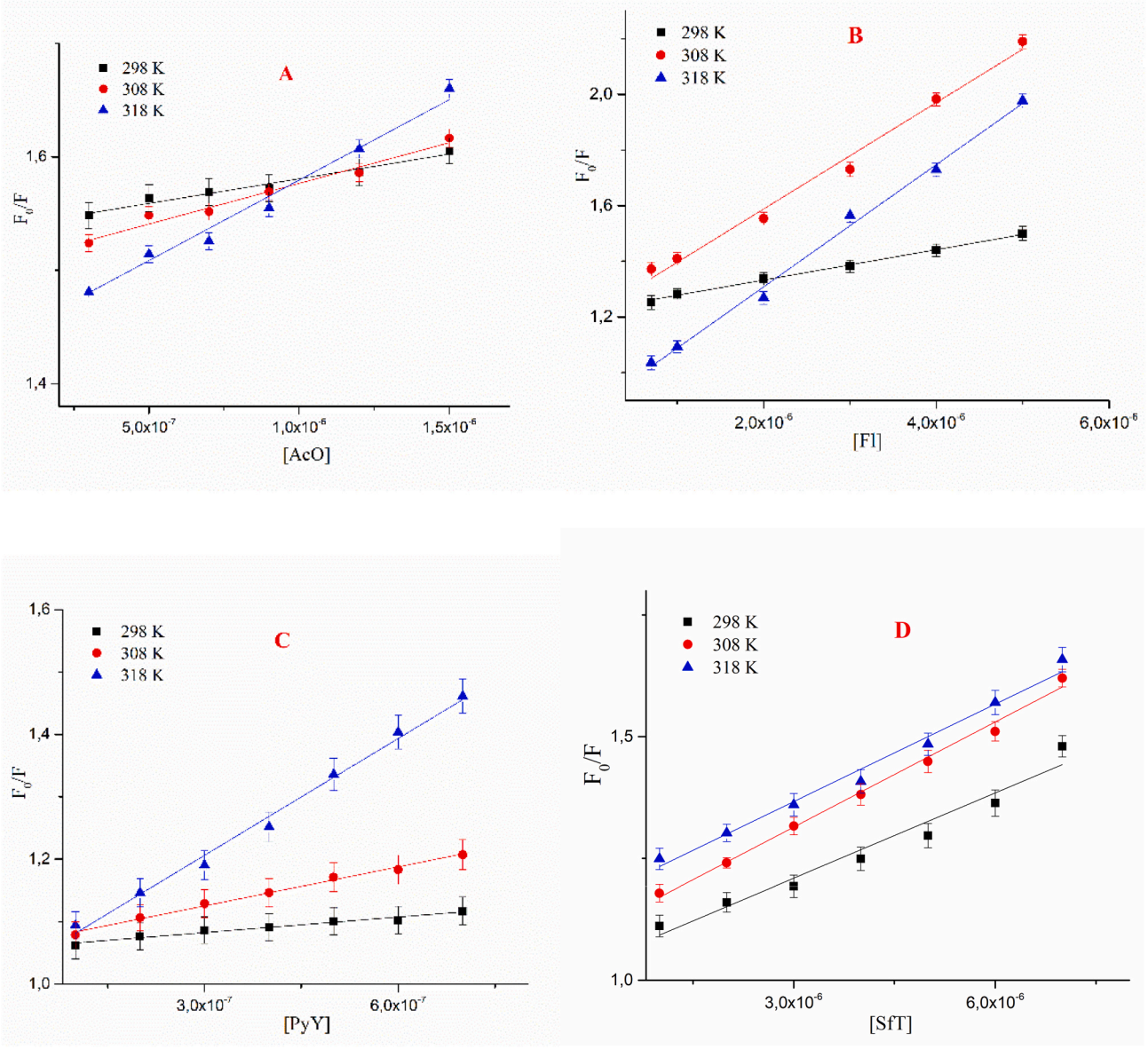


Fig. 4. Stern-Volmer plots for PDP with (A) AcO, (B) Fl, (C)PyY and (D)SfT at 298 K, 308 K and 318 K.

Table 3
Spectroscopic and photophysical parameters for PDP with Dye(s) and SDS micellar aqueous solutions.

Sample	Temperature	$K_{sv}(M^{-1})$	$k_q(M^{-1}\ s^{-1})$	$K_a(M^{-1})$	E	r(Å)	n	R^2
PyY	25 °C	1.09×10^5	2.54×10^4	2.95×10	0.092	68.92	0.987	0.852
	35 °C	1.94×10^5	4.51×10^4	1.04×10^2	0.112	66.45	0.943	0.935
	45 °C	6.55×10^5	1.52×10^5	3.31×10^4	0.223	57.94	1.131	0.938
AcO	25 °C	9.17×10^4	2.22×10^4	1.20×10^2	0.109	70.94	0.892	0.844
	35 °C	3.58×10^5	8.66×10^4	4.66×10^2	0.145	67.18	1.013	0.989
	45 °C	3.22×10^5	7.79×10^4	2.29×10	0.155	66.31	0.841	0.986
Fl	25 °C	4.73×10^4	1.12×10^4	1.31×10	0.164	65.33	0.833	0.990
	35 °C	1.78×10^4	4.21×10^3	2.77	0.179	64.19	0.711	0.949
	45 °C	1.79×10^4	4.23×10^3	2.35	0.151	66.41	0.682	0.986
SfT	25 °C	7.06×10^4	1.46×10^4	2.26×10^2	0.437	53.51	0.953	0.977
	35 °C	1.10×10^5	2.27×10^4	1.51×10^3	0.502	51.23	1.131	0.954
	45 °C	9.02×10^4	1.86×10^4	4.81×10^3	0.325	57.95	1.242	0.917

whether fluorescence quenching occurs statically or dynamically. But the linearity of the plot indicates that only one type of quenching occurs in the systems. Static and dynamic quenching can be distinguished by their different dependence on temperature or preferably by fluorescence lifetime measurements. Higher temperatures cause faster diffusion and thus larger amounts of collisional quenching. Also, higher temperature will typically result in the dissociation of weakly bonded complexes and thus smaller amounts of static quenching [33]. It can be seen that all the slopes are linear and the slope of PDP-dye(s) systems are increasing with the rising in temperatures. This shows that quenching is dynamic for

PDP- dye(s) systems.

To see the binding interaction between PDP and acceptor molecules, the relationship between fluorescence quenching intensity and quencher concentration was investigated by the double logarithm:

$$log\frac{(F_o - F)}{F} = log K_a + n\ log[Q] \quad (7)$$

where Ka: binding constant, n: refers to the number of binding sites [39,40]. The data obtained from the graphs (Fig. 5) of log ((F_o-F)) / F versus log [dye] for PDP graphs are given in Table 3. The energy transfer parameters expressed here are E: energy transfer efficiency, r: donor-acceptor distance, R^2: correlation value. Values are calculated for each temperature.

The value of K_{SV} is important in terms of providing information about the efficiency of energy transfer [33]. The large value of the Stern-Volmer rate constant is considered an indicator of the high rate of energy transfer. From the table, it is clear that the there is a strong interaction between PDP and PyY at 45 °C. The E (energy transfer efficiency) value represents the rate of energy transfer between the donor-acceptor pair. It takes a value between 0 and 1 and a value near to 1 indicates that energy transfer has occurred. In this study, the highest E value obtained was in PDP-SfT pair at 35 °C. In addition, the r values shown in the Table 3 are below 10 nm indicates that the molecules are close enough to perform the energy transfer. The n value is the number of binding sites, and the value around 1 indicates that the donor-acceptor pair interacts from a single site. The Ka value from the parameters was obtained from the double log graphs and the extent of this value indicates strong interaction between the molecules. The bimolecular quenching constant (kq) is reflects the efficiency of quenching or the accessibility of the fluorophores to the quencher. Diffusion-controlled quenching typically results in values of kq near $1 \times 10^{10}\ M^{-1}\ s^{-1}$. Values of kq smaller than the diffusion-controlled value can result from steric shielding of the fluorophore or a low quenching efficiency.

4.1.5. Fluorescence lifetime measurement studies

Since both dynamic and static quenching could exhibit a linear slope, it is difficult to distinguish these two without further information [35]. The measurement of fluorescence lifetimes is the most definitive method to distinguish static and dynamic quenching. Therefore, to elucidate the quenching mechanism, lifetime-based studies should be performed [41].

The lifetimes of PDP and PDP-dye(s) were measured using time correlated single photon counting spectroscopy with Horiba Jobin Yvon

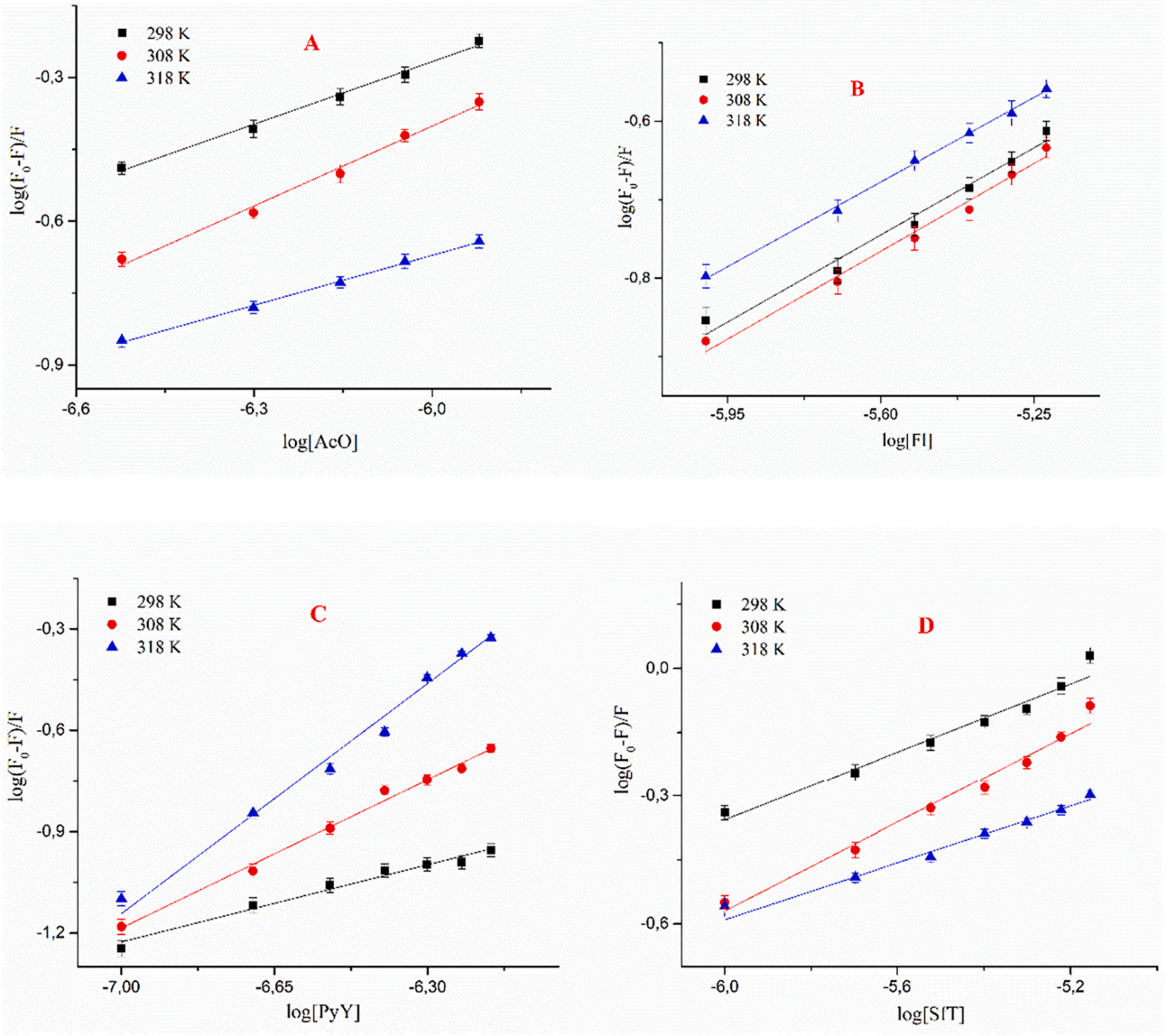


Fig. 5. Plots of the PDP quenching effect on fluorescence dyes (A) AcO, B) Fl, C) PyY, D) SfT) at 298 K, 308 K and 318 K, pH 7.4.

device measuring based on the single photon counting technique (Fig. 6) and the calculated parameters with the software are given in Table 4.

Formation of static ground-state complexes do not decrease the decay time of the uncomplexed fluorophores because only the unquenched fluorophores are observed. Dynamic quenching is a rate process acting on the entire excited-state population, and thus decreases the mean decay time of the entire excited-state population. A multi exponential decay would be observed if the donor is partially quenched by the acceptor and some of the donors do not have a nearby acceptor.

Multiple fluorescence lifetime values were obtained for PDP-dye(s) system, except for pure water, $\tau_1$and τ_2 are the shorter and longer fluorescence lifetimes and the B_1 and $B_2$are the percentages of fluorescence lifetimes, respectively. Since B_1 is more dominant than B_2, it appears that shorter lifetimes are more pronounced in PDP dye(s) systems. The table also shows $<\tau>$ and χ^2, which represent the average fluorescence lifetime, and the chi-square value, that indicates the accuracy of the measurement, respectively.

4.1.6. Thermodynamic parameters and the nature of the binding forces

We determine the thermodynamic parameters responsible for the interactions between PDP and dye compounds using Van't Hoff equation. The possible binding forces could be hydrogen bonding, van der Waals, hydrophobic and hydrophilic, and electrostatic interactions. The type of binding forces could be determined via changes in enthalpy (ΔH) and entropy (ΔS), whereas the spontaneity of the binding process could be calculated from Gibbs free energy (ΔG).

$$lnk = -\Delta H/_{RT} + \Delta S/_{R} \Delta G = \Delta H - T\Delta S = -RTlnk \quad (8)$$

According to the he Van't Hoff Equation (Eq. (4)), where K is the binding constant at the corresponding temperature; the thermodynamic parameters H and S can be calculated from the slope and intersection of linear graph, respectively. Then the Gibbs free energy (G) can be calculated from Eq. (8) [42]. Depending on the changes in enthalpy and entropy, interaction forces could be summarized as following: $\Delta H > 0$ and $\Delta S > 0$: hydrophobic forces, $\Delta H < 0$ and $\Delta S < 0$: van der Waals interactions and hydrogen bonds; $\Delta H \approx 0$ and $\Delta S > 0$: electrostatic interactions [43,44]. As can be seen in Table 5, ΔH° values are negative and ΔS° values are positive which indicate that the interaction between the donor and acceptor are essentially electrostatic in nature. In addition, the ΔG° values of the interactions of PDP and dye molecules have negative values which means that these interactions occur spontaneously.

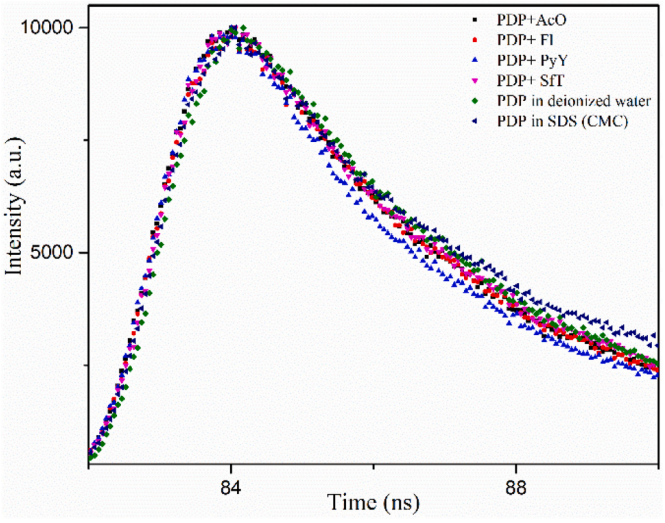


Fig. 6. Fluorescence decay profile of the interaction of PDP with AcO, SfT, PyY and Fl molecules in SDS environment.

Table 4
Fluorescence lifetime values of PDP in different environments.

Samples	τ_1(ns)	B_1(%)	τ_2(ns)	B_2(%)	$<\tau>$ (ns)	χ^2
PDP + AcO	3.384	75.20	6.411	24.80	4.134	1.503
PDP + Fl	3.700	90.20	9.084	9.80	4.227	1.428
PDP + PyY	3.187	74.10	7.474	25.90	4.297	1.783
PDP + SfT	3.650	81.17	9.974	18.83	4.840	1.639
PDP in water	4.141	100.00	–	–	4.141	1.976
PDP in SDS	3.817	66.23	1.428	33.77	3.010	1.423

Table 5
Thermodynamic parameters of the interaction of PDP with different dyes (pH = 7.40).

Dye	ΔH° (kj mol^{-1})	ΔS°(kj mol^{-1} K^{-1})	ΔG° (kj mol^{-1})
AcO	−164.44	0.56	−316.63
Fl	−74.69	0.25	−143.29
PyY	−119.24	0.41	−231.07
SfT	−53.07	0.20	−106.92

4.2. PDP-HSA interaction

4.2.1. Absorption and fluorescence spectral properties

The fluorescence techniques are widely used in bioanalytical studies for labelling proteins and DNA due to their high selectivity and unique sensitivity. Fig. 7 illustrates the absorption and fluorescence spectra of HSA and PDP in SDS media and emission spectra of HSA in the presence of PDP at various concentrations. Here we have measured FRET efficiency based on the changes in the fluorescence intensity of donor molecule rather than accepter molecules since it is more reproducible [9]. The gradual decrease in the fluorescence intensity of HSA with increasing concentrations of PDP indicates that the binding of PDP to HSA has occurred.

4.2.2. Fluorescence quantum yields

The quantum yield of HSA is shown in Table 6. It can be seen that the quantum yield of HSA is relatively high and decreases with increasing concentration PDP, indicating the occurrence of energy transfer as a result of quenching.

4.2.3. Energy transfer parameters (J and R)

We evaluated the overlap integral (J) using the overlap of the emission spectra of HSA and the absorption spectra of PDP. The R_0 and J values for PDP were found as 41.41(Å) and 6.22×10^{-14} ($M^{-1}cm^{-1}nm^4$), respectively.

4.2.4. Fluorescence quenching mechanism (Ksv, kq, Ka, E, r(Å), n, R^2)

The fluorescence measurements provide information about binding mechanism, binding mode, binding constants, binding sites, and the intermolecular distance. The fluorescence quenching data were analyzed by the Stern-Volmer equation. The Stern-Volmer plot for a PDP and HSA system at different temperatures is shown in Fig. 8. It was observed that the slope is nonlinear and it negligibly decreases with increasing temperature. K_{sv}, K_q, R^2 values were calculated from the graph and given at Table 7. It can be seen that K_{sv} and K_q values were slightly reduced with increasing temperatures. The bimolecular quenching constant (kq) is reflects the efficiency of quenching or the accessibility of the fluorophores to the quencher. Diffusion-controlled quenching typically results in values of kq near 1×10^{10} M^{-1} s^{-1}. Apparent values of kq larger than the diffusion-controlled limit usually indicate some type of binding interaction. The complex HSA and PDP appears to be persistent to composition even with increasing temperature. In addition, notably high E (energy transfer efficiency) value was observed. The E value is the energy transfer efficiency and expresses the rate of energy transfer between the donor-acceptor pair [45]. It takes a

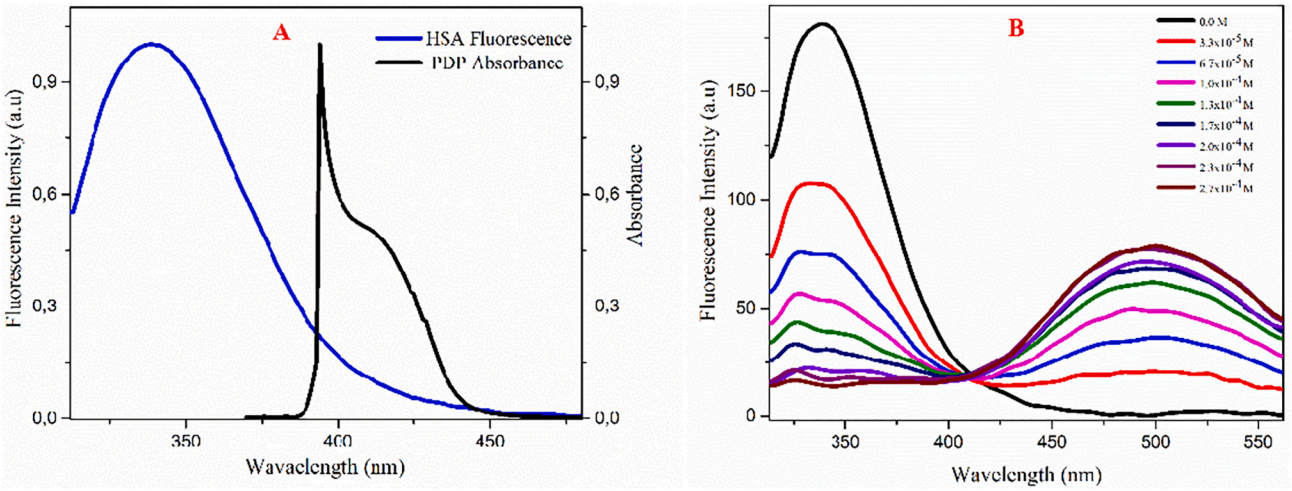


Fig. 7. A) Normalized spectral overlap spectrum of HSA fluorescence and PDP absorbance B) Representative excitation spectral profile of HSA in the presence of increasing PDP concentration

Table 6
Fluorescence quantum yields of HSA at increasing concentrations of PDP.

HSA	
[PDP] / M	ϕ_f
0	0.445 ± 0.011
3.33×10^{-5}	0.250 ± 0.004
6.67×10^{-5}	0.157 ± 0.006
1.00×10^{-4}	0.103 ± 0.011
1.33×10^{-4}	0.060 ± 0.003
1.67×10^{-4}	0.041 ± 0.007
2.00×10^{-4}	0.020 ± 0.005
2.33×10^{-4}	0.008 ± 0.005
2.67×10^{-4}	0.005 ± 0.002

value between 0 and 1, where a value close to 1 means that energy transfer has occurred. The average binding distance between HSA and PDP was estimated about ≈ 3.6 nm at all temperatures suggesting that the energy transfer occurs well in the range and it is reliable to use FRET in the complex of these two molecules. The molar ratio of the complex formed is around 1:1, suggesting that one mole of HSA binds to one mole of PDP.

4.2.5. *Fluorescence lifetime measurement studies*

The fluorescence lifetimes of PDP and PDP -HSA pair were recorded using time correlated single photon counting spectroscopy (Fig. 9). In general, the fluorescence lifetime τ_0 of HSA was reported approximately as 10^{-8} s [49].The shorter (τ_1) and the longer (τ_2) fluorescence lifetimes values of HSA were obtained as 3.446 ns and 5.341 ns, respectively. Since B_1 (64.27) is greater than B_2 (35.73), it is clear that the shorter lifetimes are more apparent in HSA-PDP system (χ^2: 1.511).

4.2.6. *Thermodynamic parameters and the nature of the binding forces*

We also calculated thermodynamic parameters for HSA and PDP. The data indicates that both ΔG (−15.09 kj mol^{-1}) and ΔH (−4.87 kj mol^{-1}) were negative which means that the complex formation is spontaneous and the reaction is exothermic. As ΔS (0.04 kj mol^{-1} K^{-1}) were positive, it can be concluded that the binding process occurs via both hydrophobic and electrostatic interactions (pH = 7.4).

4.3. *Cytotoxicity*

Cytotoxicity studies have been accepted as an obligatory step to introduce a newly synthesized chemical compound to the pharmaceutical industry as well as evaluating for different intents in the biological

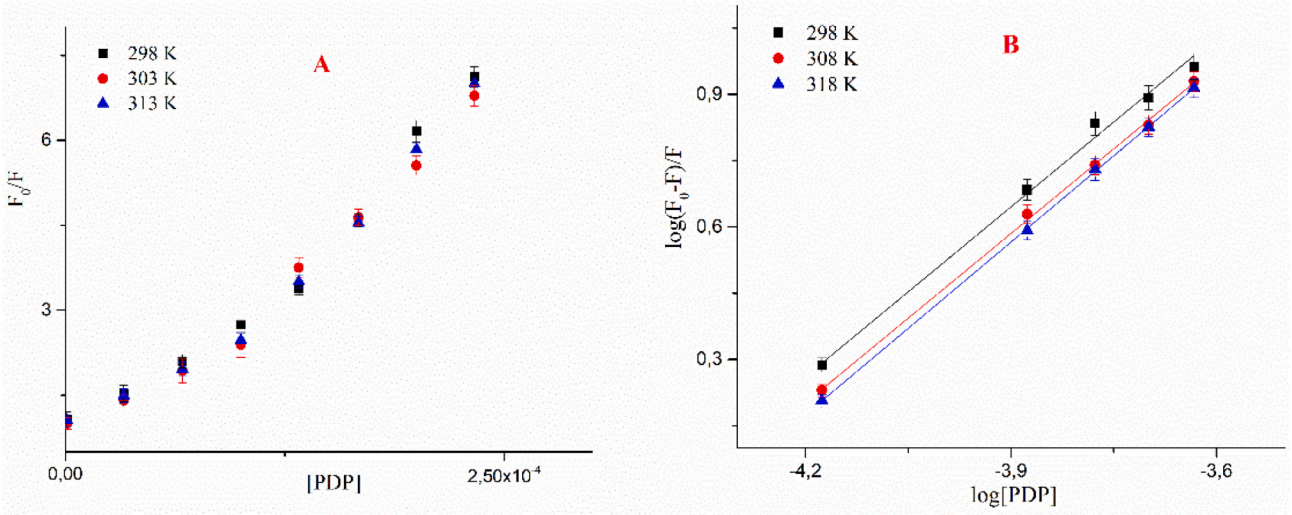


Fig. 8. A) Stern-Volmer plot and B) Logarithmic plot of HSA quenching effect PDP at 298 K, 308 K and 318 K, pH 7.4. [HSA] = 1.0 mol L^{-1}, λex = 290 nm; λem = 305–570 nm.

Table 7
Stern-Volmer association constants(K_{sv}), quenching constants(k_q), Binding constants(Kb), energy transfer efficiency(E), donor-acceptor distance(r) and number of binding site(n), parameters of the interaction of PDP with HSA at different temperature (pH = 7.4).

Temperature	$K_{sv}(M^{-1})$	$k_q(M^{-1}\ s^{-1})$	$K_a(M^{-1})$	E	r(Å)	n	R^2
25 °C	2.64×10^4	2.64×10^{12}	1.13×10^5	0.710	35.67	1.129	0.960
35 °C	2.53×10^4	2.53×10^{12}	1.13×10^5	0.691	36.21	1.145	0.971
45 °C	2.58×10^4	2.58×10^{12}	1.31×10^5	0.701	35.93	1.169	0.961

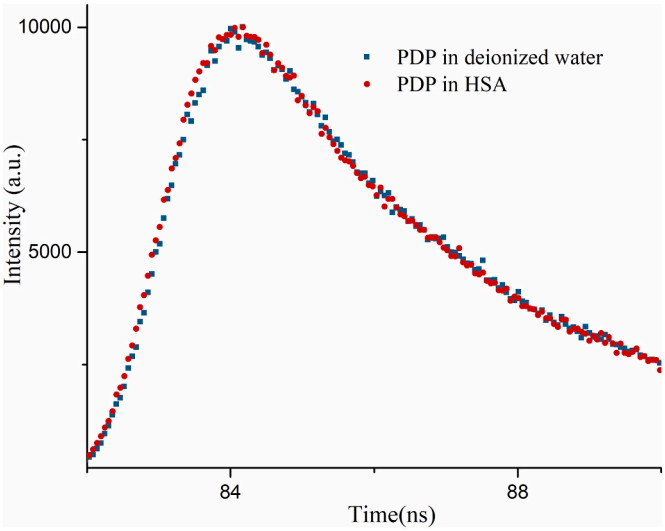


Fig. 9. Fluorescence decay profile of HSA–PDP. [HSA] = 1.0×10^{-6} M; λex = 290 nm; λem = 305–570 nm and pH = 7.4

systems, including the cell staining feature of a probe [46]. As seen in Fig. 10, our results showed that PDP showed no statistically significant changes in the proliferation of MCF-7 cells at 100 μM ($p > 0.05$) compared to the control group cells. However, when the concentration was increased to 250 μM, it was observed a 22% inhibition (**$p < 0.01$). For the HT-29 cell line, the compound at 100 μM caused an increase in cell proliferation compared to the control group (*$p < 0.05$), while it did not cause a statistically significant change at 250 μM ($p > 0.05$). As for healthy 3 T3-L1cell line, the compound did not cause any significant change in cell proliferation at 100 μM ($p > 0.05$), but it caused a statistical significant inhibition at 250 μM (*$p < 0.05$). All these data reveal that PDP does not have any cytotoxic effect at the concentration of 100 μM on both cancer and healthy cell lines. On the other hand, when the concentration is reached to 250 μM, it still does not have any significant effect on HT-29 cancer cells, but has a moderate cytotoxicity against MCF-7 and 3 T3-L1 cells.

4.4. Confocal microscope examination

The light microscopes are useful in understanding the morphology of the cell; however, it is limited to provide information about the function and biophysical events in intact cells. The combination of confocal microscopes with FRET technique, it is now possible to monitor directly the interactions of proteins with specific macromolecules in the natural environments of the cells [47,48]. Therefore, in this study, we looked at whether PDP is taken up by the cell and could be used to stain the cells. Confocal images of breast cancer cell line are shown in Fig. 11. Examination of confocal fluorescence images reveals that PDP stains the cytoplasm of breast cancer cells. The merged image shows that only the cytoplasm of the cells is stained. The images obtained prove that PDP can be used for cell staining.

5. Conclusion

In summary, PDP was synthesized and characterized, and the FRET capacity of PDP in the medium of SDS micelle and HSA was investigated spectroscopically. In addition, the cytotoxic effects of PDP were investigated using three different cell lines and confocal images of breast cancer cells were monitored to test whether PDP could be used to stain the cell cytoplasm. The result showed that PDP is an efficient donor molecule for dyes (AcO, Fl, PyY and SfT) and a considerable acceptor for HSA, as evidenced by FRET studies. The interactions were spontaneous and electrostatic in nature. The cytotoxic activity studies showed that PDP at 100 μM did not exhibit antiproliferative activity against the tested cancer and healthy cell lines. Thus, these results clearly demonstrate that the molecule can be used at these concentration ranges for both fluorescence imaging and cell staining.

Fundings

This work supported by Research Foundation of Erzincan Binali Yıldırım University (grant number: FYL-2019-597), and Scientific and Technologic Research Foundation of Turkey (TUBITAK), grant number: 113R010).

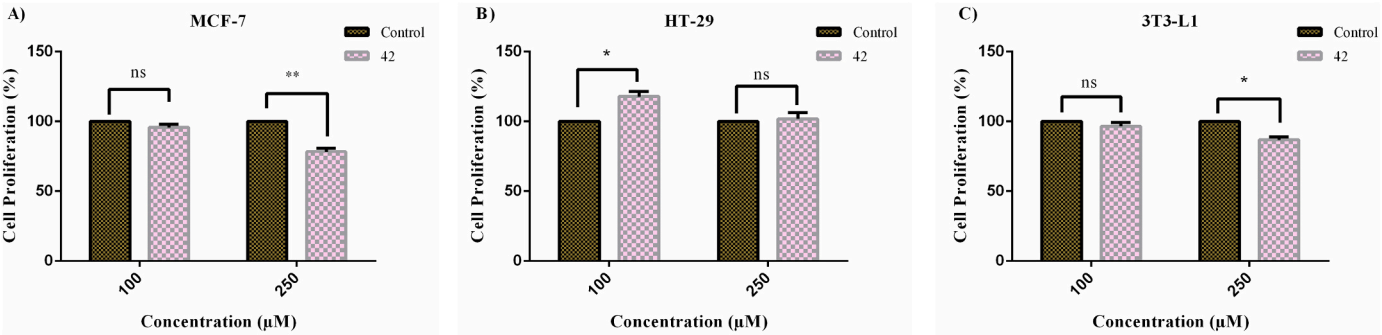


Fig. 10. The cytotoxicity of the compound PDP) against human breast adenocarcinoma MCF-7 (A), colorectal adenocarcinoma HT-29 (B) and non-carcinogenic mouse fibroblast 3 T3-L1 (C) cell lines. All the cell lines were exposed to the compound (PDP) for 24 h. Each experiment was applied as triplicate, ns(non-significant); *p < 0.05 (significant); **p < 0.01 (highly significant).

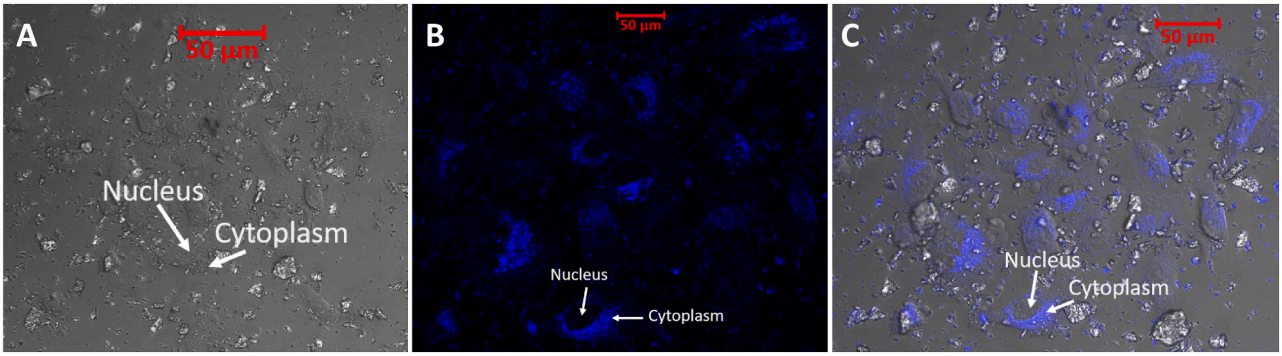


Fig. 11. Standard light microscopy image (A), fluorescence microscopy image (B) and overlay of fluorescence and light microscopy image (C) of MCF-7 cell lines.

CRediT authorship contribution statement

Berat Yildirim: Investigation. **Burcu Meryem Beşer:** Conceptualization, Methodology, Funding acquisition, Validation, Data curation, Writing – original draft. **Nevin Ulaş Çolak:** Investigation. **Ahmet Altay:** Investigation, Data curation. **Ahmet Yaşar:** Funding acquisition, Methodology, Data curation.

Declaration of Competing Interest

The authors declare that they have no known competing financial interests or personal relationships that could have appeared to influence the work reported in this paper.

Appendix A. Supplementary data

Supplementary data to this article can be found online at https://doi.org/10.1016/j.bpc.2022.106879.

References

[1] H. Apotheker, O. Osman, First Contact Imaging of Nanoparticular siRNA – From Synthesis to Application of a Prodye Concept, 2015.
[2] S. Syam, S.I. Abdelwahab, M.A. Al-Mamary, S. Mohan, Synthesis of chalcones with anticancer activities, Molecules 17 (2012) 6179–6195, https://doi.org/10.3390/molecules17066179.
[3] R. Sharma, R. Kumar, R. Kodwani, S. Kapoor, A. Khare, R. Bansal, et al., A Review on Mechanisms of Anti Tumor Activity of Chalcones, Anti Cancer Agents Med. Chem. 16 (2015) 200–211, https://doi.org/10.2174/1871520615666150518093144.
[4] S. Tekale, S. Mashele, O. Pooe, S. Thore, P. Kendrekar, R. Pawar, Biological role of chalcones in medicinal chemistry, Vector-Borne Dis. Recent Dev. Epidemiol. Control (2020), https://doi.org/10.5772/intechopen.91626.
[5] D. Batovska, I. Todorova, Trends in utilization of the pharmacological potential of chalcones, Curr. Clin. Pharmacol. 5 (2010) 1–29, https://doi.org/10.2174/157488410790410579.
[6] B. Salehi, C. Quispe, I. Chamkhi, N. El Omari, A. Balahbib, J. Sharifi-Rad, et al., Pharmacological properties of chalcones: a review of preclinical including molecular mechanisms and clinical evidence, Front. Pharmacol. 11 (2021), https://doi.org/10.3389/fphar.2020.592654.
[7] H. Suwito, J. Jumina, M. Mustofa, A.N. Kristanti, N.N. Tri Puspaningsih, ChemInform abstract: chalcones: synthesis, structure diversity and pharmacological aspects, ChemInform 46 (2015), https://doi.org/10.1002/chin.201507329.
[8] A. Yaşar, N. Ulaş, S. Yıldırım, Microwave assisted synthesis of 2′−/ 3′-azaflavones/azaflavonones and their N-alkyl derivatives, Org. Commun. 4 (2016) 73–81.
[9] P. Banerjee, S. Pramanik, A. Sarkar, S.C. Bhattacharya, Deciphering the fluorescence resonance energy transfer signature of 3-pyrazolyl 2-pyrazoline in transport proteinous environment, J. Phys. Chem. B 113 (2009) 11429–11436, https://doi.org/10.1021/jp811479r.
[10] E.A. Jares-Erijman, T.M. Jovin, Imaging molecular interactions in living cells by FRET microscopy, Curr. Opin. Chem. Biol. 10 (2006) 409–416, https://doi.org/10.1016/j.cbpa.2006.08.021.
[11] R.B. Sekar, A. Periasamy, Fluorescence resonance energy transfer (FRET) microscopy imaging of live cell protein localizations, J. Cell Biol. 160 (2003) 629–633, https://doi.org/10.1083/JCB.200210140.
[12] A. Roy, N. Kundu, D. Banik, N. Sarkar, Comparative fluorescence resonance energy-transfer study in pluronic triblock copolymer micelle and niosome composed of biological component cholesterol: an investigation of effect of cholesterol and sucrose on the FRET parameters, J. Phys. Chem. B 120 (2016) 131–142, https://doi.org/10.1021/acs.jpcb.5b09761.
[13] M.F. Nazar, S.S. Shah, M.A. Khosa, Interaction of azo dye with cationic surfactant under different pH conditions, J. Surfactant Deterg. 13 (2010) 529–537, https://doi.org/10.1007/s11743-009-1177-8.
[14] S. Ghosh, A. Ray, N. Pramanik, Self-assembly of surfactants: an overview on general aspects of amphiphiles, Biophys. Chem. 265 (2020), 106429, https://doi.org/10.1016/j.bpc.2020.106429.
[15] U.H.N. Dürr, M. Gildenberg, A. Ramamoorthy, The magic of bicelles lights up membrane protein structure, Chem. Rev. 112 (2012) 6054–6074, https://doi.org/10.1021/cr300061w.
[16] J.C. Bozelli, S.S. Aulakh, R.M. Epand, Membrane shape as determinant of protein properties, Biophys. Chem. 273 (2021), https://doi.org/10.1016/j.bpc.2021.106587.
[17] F. Szoka, Comparação Métdos De Preparo, 1980, pp. 467–508.
[18] D.S. Pellosi, I.R. Calori, L.B. de Paula, N. Hioka, F. Quaglia, A.C. Tedesco, Multifunctional theranostic Pluronic mixed micelles improve targeted photoactivity of Verteporfin in cancer cells, Mater. Sci. Eng. C 71 (2017) 1–9, https://doi.org/10.1016/j.msec.2016.09.064.
[19] Z. Chai, D. Ran, L. Lu, C. Zhan, H. Ruan, X. Hu, et al., Ligand-modified cell membrane enables the targeted delivery of drug nanocrystals to glioma, ACS Nano 13 (2019) 5591–5601, https://doi.org/10.1021/acsnano.9b00661.
[20] P.G. Pronkin, L.A. Shvedova, A.S. Tatikolov, Comparative study of the interaction of some meso-substituted anionic cyanine dyes with human serum albumin, Biophys. Chem. 261 (2020), 106378, https://doi.org/10.1016/j.bpc.2020.106378.
[21] K. Ganorkar, S. Mukherjee, P. Singh, S.K. Ghosh, Stabilization of a potential anticancer thiosemicarbazone derivative in Sudlow site I of human serum albumin: In vitro spectroscopy coupled with molecular dynamics simulation, Biophys. Chem. 269 (2021), 106509, https://doi.org/10.1016/j.bpc.2020.106509.
[22] F. Ge, C. Chen, D. Liu, B. Han, X. Xiong, S. Zhao, Study on the interaction between theasinesin and human serum albumin by fluorescence spectroscopy, J. Lumin. 130 (2010) 168–173, https://doi.org/10.1016/j.jlumin.2009.08.003.
[23] C. Liao, F. Li, S. Huang, B. Zheng, J. Du, D. Xiao, A specific and biocompatible fluorescent sensor based on the hybrid of GFP chromophore and peptide for HSA detection, Biosens. Bioelectron. 86 (2016) 489–495, https://doi.org/10.1016/j.bios.2016.07.002.
[24] K. Martinez Pomier, R. Ahmed, G. Melacini, Interactions of intrinsically disordered proteins with the unconventional chaperone human serum albumin: From mechanisms of amyloid inhibition to therapeutic opportunities, Biophys. Chem. 282 (2022), 106743, https://doi.org/10.1016/j.bpc.2021.106743.
[25] C. Liu, W. Yang, Q. Gao, J. Du, H. Luo, Y. Liu, et al., Differential recognition and quantification of HSA and BSA based on two red-NIR fluorescent probes, J. Lumin. 197 (2018) 193–199, https://doi.org/10.1016/j.jlumin.2018.01.021.
[26] S. Ghosh, D. Singharoy, S.C. Bhattacharya, Spectroscopic and theoretical investigation of conformational changes of proteins by synthesized pyrimidine derivative and its sensitivity towards FRET application, Spectrochim. Acta - Part A Mol. Biomol. Spectrosc. 195 (2018) 7–15, https://doi.org/10.1016/j.saa.2018.01.029.
[27] S. Rudra, S. Dasmandal, C. Patra, B.K. Patel, S. Paul, A. Mahapatra, Characterization of domain-specific interaction of synthesized dye with serum proteins by spectroscopic and docking approaches along with determination of in vitro cytotoxicity and antiviral activity, J. Biomol. Struct. Dyn. 36 (2018) 3773–3790, https://doi.org/10.1080/07391102.2017.1400468.
[28] V. Lanza, N. Licciardello, F. Laneri, S. García-vi, S. Sortino, G. Grasso, Dipyridamole for tracking amyloidogenic proteins aggregation and enhancing polyubiquitination 728, 2022, https://doi.org/10.1016/j.abb.2022.109354.
[29] H. Xiong, Y. Wu, Z. Jiang, J. Zhou, M. Yang, J. Yao, pH-activatable polymeric nanodrugs enhanced tumor chemo/antiangiogenic combination therapy through improving targeting drug release, J. Colloid Interface Sci. 536 (2019) 135–148, https://doi.org/10.1016/j.jcis.2018.10.039.
[30] M. Persico, S. García-Viñuales, A.M. Santoro, V. Lanza, G.R. Tundo, D. Sbardella, et al., Silybins are stereospecific regulators of the 20S proteasome, Bioorg. Med. Chem. 66 (2022), https://doi.org/10.1016/j.bmc.2022.116813.
[31] S. García-Viñuales, I.M. Ilie, A.M. Santoro, V. Romanucci, A. Zarrelli, G. Di Fabio, et al., Silybins inhibit human IAPP amyloid growth and toxicity through

stereospecific interactions, Biochim. Biophys. Acta, Proteins Proteomics 2022 (1870), https://doi.org/10.1016/j.bbapap.2022.140772.
[32] S. Fery-Forgues, D. Lavabre, Are fluorescence quantum yields so tricky to measure? A demonstration using familiar stationery products, J. Chem. Educ. 76 (1999) 1260–1264, https://doi.org/10.1021/ed076p1260.
[33] J.R. Lakowicz, Principles of Fluorescence Spectroscopy Principles of Fluorescence Spectroscopy, 2006, https://doi.org/10.1007/978-0-387-46312-4.
[34] S. Aygün, B.M. Beşer, M. Acar, K. Meral, Photophysical properties of some fluorescent dyes in SDS micellar solutions, J. Fluoresc. 30 (2020) 849–857, https://doi.org/10.1007/s10895-020-02553-8.
[35] A.M. Brouwer, Standards for photoluminescence quantum yield measurements in solution (IUPAC technical report), Pure Appl. Chem. 83 (2011) 2213–2228, https://doi.org/10.1351/PAC-REP-10-09-31.
[36] B.M. Aydin, M. Acar, M. Arik, Y. Onganer, The fluorescence resonance energy transfer between dye compounds in micellar media, Dyes Pigments 81 (2009) 156–160, https://doi.org/10.1016/j.dyepig.2008.10.002.
[37] Y. Arai, T. Nagai, Extensive use of FRET in biological imaging, J. Electron Microsc. 62 (2013) 419–428, https://doi.org/10.1093/jmicro/dft037.
[38] K. Ghosh, S. Rathi, D. Arora, Fluorescence spectral studies on interaction of fluorescent probes with Bovine Serum Albumin (BSA), J. Lumin. 175 (2016) 135–140, https://doi.org/10.1016/j.jlumin.2016.01.029.
[39] S. Roy, Das T. Kumar, Investigation of interaction between casein enzyme hydrolysate and biosynthesized silver nanoparticles by spectroscopy, Nanosci. Nanotechnol. Lett. 6 (2014) 547–554, https://doi.org/10.1166/nnl.2014.1852.
[40] J. Xiao, X. Wei, Y. Wang, C. Liu, Fluorescence resonance energy-transfer affects the determination of the affinity between ligand and proteins obtained by fluorescence quenching method, Spectrochim. Acta - Part A Mol. Biomol. Spectrosc. 74 (2009) 977–982, https://doi.org/10.1016/j.saa.2009.09.003.
[41] J.H. Wosnick, R.W. Field, Supervisor, 2004.
[42] S. Roy, S. Ponra, R.K. Nandi, K.C. Majumdar, T.K. Das, Biophysical study on the interaction of spirooxindole-annulated thiopyran derivatives with bovine serum albumin using spectroscopic and docking methods, Adv. Mater. Lett. 6 (2015) 913–919, https://doi.org/10.5185/amlett.2015.5931.
[43] J.J.J. Li, J.J.J. Li, Y. Jiao, C. Dong, S. Afzal, M.S. Lone, et al., Selective fluorescence resonance energy transfer from serum albumins to a bio-active 3-pyrazolyl-2-pyrazoline derivative: a spectroscopic analysis, Spectrochim. Acta - Part A Mol. Biomol. Spectrosc. 6 (2012) 2612–2618, https://doi.org/10.1016/j.lfs.2016.02.048.
[44] T. Wang, B.R. Xiang, Y. Li, C.Y. Chen, X.H. Zhou, Z.M. Wang, et al., Studies on the binding of a carditionic agent to human serum albumin by two-dimensional correlation fluorescence spectroscopy and molecular modeling, J. Mol. Struct. 921 (2009) 188–198, https://doi.org/10.1016/j.molstruc.2008.12.047.
[45] S. Afzal, M.S. Lone, P.A. Bhat, A.A. Dar, Multi-step fluorescence resonance energy transfer between the fluorophores via cosolubilization in cationic, anionic and non-ionic micelles, J. Photochem. Photobiol. A Chem. 365 (2018) 220–231, https://doi.org/10.1016/j.jphotochem.2018.08.002.
[46] S.J. Gawandi, V.G. Desai, S.G. Shingade, Design, synthesis, and biological evaluation of 1,3,5-trisubstituted pyrazoles as tyrosine kinase inhibitors, Med. Chem. Res. 28 (2019) 267–278, https://doi.org/10.1007/s00044-018-2282-x.
[47] B.M. Beşer, A. Altay, O. Talaz, B. Türkmenoğlu, A bis indole analog molecule fluorescent probe for living cell staining, J. Photochem. Photobiol. A Chem. 424 (2022), 113613, https://doi.org/10.1016/J.JPHOTOCHEM.2021.113613.
[48] J. Goedhart, D. Von Stetten, M. Noirclerc-Savoye, M. Lelimousin, L. Joosen, M. A. Hink, et al., Structure-guided evolution of cyan fluorescent proteins towards a quantum yield of 93%, Nat. Commun. (2012) https://doi.org/10.1038/ncomms1738.
[49] Girish G. Ariga, Praveen N. Naik, Shivamurti A. Chimatadar, Sharanappa T. Nandibewoor, Interactions between epinastine and human serum albumin: Investigation by fluorescence, UVevis, FTeIR, CD, lifetime measurement and molecular docking, J. Mol. Struct. 1137 (2017) 485–494 46, https://doi.org/10.1016/j.molstruc.2016.12.066. In preparation.